RESEARCH ARTICLE

Key Points:
- MHD model can reproduce magnetospheric expansion during long-lasting radial IMF intervals
- We change solar wind boundary conditions in simulations based on previous observations in the foreshock cavity
- The strong total pressure decrease in the magnetosheath is a local, rather than a global, phenomenon

Correspondence to:
A. A. Samsonov,
a.samsonov@spbu.ru

A method to predict magnetopause expansion in radial IMF events by MHD simulations

A. A. Samsonov[1] iD, **D. G. Sibeck**[2] iD, **J. Šafránková**[3], **Z. Němeček**[3], and **J.-H. Shue**[4] iD

[1]Saint Petersburg State University, Saint Petersburg, Russia, [2]Code 674, NASA Goddard Space Flight Center, Greenbelt, Maryland, USA, [3]Faculty of Mathematics and Physics, Charles University, Prague, Czech Republic, [4]Institute of Space Science, National Central University, Jhongli, Taiwan

Abstract This paper presents a method for taking into account changes of solar wind parameters in the foreshock using global MHD simulations. We simulate four events with very distant subsolar magnetopause crossings that occurred during quasi-radial interplanetary magnetic field (IMF) intervals lasting from one to several hours. Using previous statistical results, we suggest that the density and velocity in the foreshock cavity decrease to ~60% and ~94% of the ambient solar wind values when the IMF cone angle falls below 50°. This diminishes the solar wind dynamic pressure to 53% and causes a corresponding magnetospheric expansion. We change the upstream solar wind parameters in a global MHD model to take these foreshock effects into account. We demonstrate that the modified model predicts magnetopause distances during radial IMF intervals close to those observed by THEMIS. The strong total pressure decrease in the data seems to be a local, rather than a global, phenomenon. Although the simulations with decreased solar wind pressure generally reproduce the observed total pressure in the magnetosheath well, the total pressure in the magnetosphere often agrees better with results for nonmodified boundary conditions. The last result reveals a limitation of our method: we changed the boundary conditions along the whole inflow boundary, although a more correct approach would be to vary parameters only in the foreshock. A model with the suggested global modification of the boundary conditions better predicts the location of part of the magnetopause behind the foreshock but may fail in predicting the rest of the magnetopause.

1. Introduction

The magnitude and orientation of the interplanetary magnetic field (IMF) as well as the solar wind velocity are the most important factors controlling geomagnetic activity. Typical "educational" cases with steady northward, southward, and eastward (westward) IMF orientations have been well studied using global magnetospheric models, and a relatively large number of observations for such solar wind conditions are available. On the contrary, cases when the IMF direction points radially outward from the Sun (or toward the Sun) and lies nearly aligned with the solar wind velocity occur rarely, and numerical simulations of such events may encounter large difficulties both because kinetic effects become very important [*Karimabadi et al.*, 2014; *Palmroth et al.*, 2015] and because a shift of the solar wind data from L 1 point to the bow shock nose is not straightforward, as will be shown below.

Early satellite observations of the foreshock showed a diffuse population of hot solar wind ions energized by Fermi acceleration outside the bow shock [e.g., *Greenstadt et al.*, 1968; *Asbridge et al.*, 1968]. This population usually forms when the angle between the IMF direction and the shock normal is small. This foreshock region generates compressional magnetosonic waves in the Pc 3–4 range (~10–100 s) that also can be observed in magnetospheric and ground data [*Troitskaya et al.*, 1971; *Paschmann et al.*, 1979; *Engebretson et al.*, 1987; *Fairfield et al.*, 1990]. *Fairfield et al.* [1990] first suggested that an extended foreshock may expedite the solar wind flow around the magnetosphere and diminish the solar wind pressure applied to the subsolar magnetopause. This suggestion was later confirmed in several radial IMF events [*Merka et al.*, 2003; *Jelínek et al.*, 2010; *Suvorova et al.*, 2010].

Merka et al. [2003] considered a long radial IMF interval on 5 May 1996 when the angle between the IMF and solar wind velocity was only 15°. In this interval, the subsolar magnetopause crossing was observed ~$2\,R_E$ farther outward than predicted by the *Shue et al.* [1998] model, while the magnetosheath was unusually thin, at most 10% of the magnetopause standoff distance. *Jelínek et al.* [2010] studied an event on 16 July 2007

observed by five THEMIS probes in the dayside magnetosphere/magnetosheath, by Geotail in the flank magnetosheath, and by ACE and Wind near L1 in the upstream solar wind. The THEMIS spacecraft were at different radial distances from the Earth ranging approximately from 11 to 13 R_E and observed multiple magnetopause crossings, while neither ACE nor Wind observed significant variations in the solar wind dynamic pressure or IMF B_z, but the IMF cone angle θ_{BX} (the angle between the IMF and the x GSE axis) observed by ACE fell below 30°. The IMF cone angle at Wind fell below 30° during the first half of the interval but varied between 30° and 50° in the second half. Energy spectra and magnetic fields observed by THEMIS and Geotail in the magnetosheath suggested that the spacecraft were located downstream from the quasi-parallel bow shock.

Suvorova et al. [2010] considered three radial events, and one of them was again the event on 16 July 2007. They compared observed magnetopause crossings in this event with predictions of the *Shue et al.* [1998] model and found that the model underestimated the magnetopause distance by ∼2 R_E. *Suvorova et al.* [2010] also showed that the ratio of total magnetosheath to solar wind pressure remains below 0.5; therefore, they called such conditions a low-pressure magnetosheath (LPM) mode. Both *Jelínek et al.* [2010] and *Suvorova et al.* [2010] noted that the large magnetopause displacement was connected with a significant distortion of the magnetopause surface. Observations of large magnetopause distortions and anomalous sunward magnetosheath flows in another radial event were presented by *Shue et al.* [2009].

Magnetopause expansion for nearly radial IMF was also demonstrated in a statistical study based on ≃6500 magnetopause crossings [*Dušík et al.*, 2010] or on magnetic fields obtained from Geostationary Operational Environmental Satellites (GOES) [*Park et al.*, 2016]. Their results showed a systematic increase of observed magnetopause distances for radial IMF conditions, from ≃0.3 R_E at 90° to ≃1.7 R_E at 0° or 180° cone angles with respect to empirical models. *Suvorova and Dmitriev* [2015] inspected the ability of empirical magnetopause models to predict the magnetospheric expansion and found that only 4 out of 14 models, namely, *Pudovkin et al.* [1998], *Kuznetsov and Suvorova* [1998], *Suvorova et al.* [1999], and *Lin et al.* [2010], could predict magnetopause positions for extremely low pressures and, hence, can be useful for quantitative estimation of the magnetospheric expansion under quasi-radial IMF orientation.

Samsonov et al. [2012] suggested an explanation for the observed magnetopause expansion and the LPM mode initiation. First, they showed that the total pressure varies across the magnetosheath and these variations depend on the IMF orientation. In the purely hydrodynamic (with $B = 0$) and radial IMF cases, the total pressure decreases from the bow shock to the magnetopause by ∼12%, while a magnetic barrier that formed ahead of the magnetopause in the northward IMF case increases the total pressure, and therefore, the pressure at the subsolar point differs only slightly from the solar wind pressure. Second, *Samsonov et al.* [2012] found that the difference between the radial and northward cases becomes larger in the anisotropic MHD simulation than in the isotropic one. Thus, the anisotropic MHD model can explain a total pressure decrease through the magnetosheath to ∼76%. *Samsonov et al.* [2012] also noted that observed positions of the magnetopause in radial events are not stationary, and therefore, the magnetopause may be farther or closer to the Earth due to the oscillations.

However, the MHD simulations of *Samsonov et al.* [2012] do not take into account the foreshock effect. Reflected solar wind ions in the foreshock region can decrease the solar wind density and velocity near the quasi-parallel bow shock. Moreover, this effect has been quantified in observations [*Sibeck et al.*, 2001]. Statistical results from Cluster [*Billingham et al.*, 2008] show that the density in foreshock cavities is on the average only 60% of surrounding solar wind density. The solar wind velocity in the foreshock also decreases, but these changes, according to their estimations, do not exceed several percent. The largest velocity decrease reaches 22 km/s [*Cao et al.*, 2009] or 94% of surrounding values [*Urbar et al.*, 2013]. The situation may be more complicated when foreshock bubbles form [e.g., *Omidi et al.*, 2010; *Turner et al.*, 2013; *Archer et al.*, 2015]. The bubbles are transient phenomena resulting from the interaction of suprathermal backstreaming ions with a discontinuity and have sizes up to ≃10 R_E or more. However, we do not consider inhomogeneities in the foreshock cavity in our method described below.

The purpose of our paper is to reproduce magnetospheric expansions during several long-lasting radial IMF events with a numerical MHD model by modifying solar wind boundary conditions. Since MHD models do not account for foreshock kinetic effects, we use the statistical results obtained by *Billingham et al.* [2008], *Cao et al.* [2009], and *Urbar et al.* [2013] showing the density and velocity decreases in the foreshock cavity. We will

check that (1) the model is able to predict observed magnetopause crossings and (2) the total pressure in the magnetosheath obtained in simulations agrees with observations.

We have first reproduced the event on 16 July 2007 studied before by *Jelínek et al.* [2010] and *Suvorova et al.* [2010], because this is a long radial IMF interval in which the position of the subsolar magnetopause was well determined by the five THEMIS spacecraft, while the upstream solar wind conditions were obtained from both ACE and Wind. Note also that the geomagnetic activity was low in this case; therefore, we do not expect inner magnetospheric processes to influence the magnetopause position. Second, in order to verify our approach, we have extended our study and simulated three more events. Since the method is based on the reduction of the upstream pressure, we have chosen events differing by this pressure. The range is not too broad (0.6–1.3 nPa), and it is shifted toward values lower than an expected average value in accord with the finding that the average solar wind dynamic pressure is weaker during intervals of radial IMF [*Pi et al.*, 2014]. Skipping small-scale variations, we conclude that our method generally reproduces magnetospheric expansions and total pressure reductions in the dayside magnetosheath during radial IMF intervals.

2. Data Sets and MHD Model

We use both ACE and Wind solar wind monitors to determine input conditions for MHD simulations. In particular, we use data from the Magnetic Field Instrument (MAG) [*Smith et al.*, 1998] and Solar Wind Electron Proton Alpha Monitor (SWEPAM) [*McComas et al.*, 1998] on ACE and from the Magnetic Field Investigation (MFI) [*Lepping et al.*, 1995] and Solar Wind Experiment (SWE) [*Ogilvie et al.*, 1995] on Wind.

We use THEMIS magnetic field data from the Flux Gate Magnetometer (FGM) [*Auster et al.*, 2008], and ion density and velocities from the Electrostatic Analyzer (ESA) [*McFadden et al.*, 2008]. For the event on 16 July 2007, we also use the Comprehensive Plasma Instrument (CPI) [*Frank et al.*, 1994] and Magnetic Field Instrument (MGF) [*Kokubun et al.*, 1994] on Geotail, and the Fluxgate magnetometer data (MAG) on GOES 11.

For the simulations below, we use the Space Weather Modeling Framework (SWMF) global MHD model (former BATS-R-US) [*Tóth et al.*, 2005, 2012] available through Community Coordinated Modeling Center (CCMC) runs on request. Note that other global MHD models whose results can be obtained through CCMC runs (LFM, OpenGGCM) predict even smaller subsolar magnetopause distances (as noted by *Samsonov et al.* [2016]). MHD models coupled with inner magnetosphere codes (e.g., BATS-R-US with CRCM) predict a slightly larger magnetopause distance, but the difference in magnetopause position between BATS-R-US and BATS-R-US coupled with RCM/CRCM is about one order smaller than the difference resulting from modification of boundary conditions as explained below. In our runs, we have used grids with a typical spatial resolution near the dayside magnetopause of 0.25 R_E. For the event on 16 July 2007, we have compared results of a standard BATS-R-US run with a high-resolution run (0.125 R_E in the dayside magnetosphere) and with two other standard resolution runs but using BATS-R-US coupled with RCM and CRCM. Neither BATS-R-US with RCM/CRCM nor BATS-R-US with the higher-resolution grid improves the numerical predictions for comparison with observations. The magnetopause position in the simulations was determined as the boundary of closed field lines, and it approximately coincides with maxima of the density gradient and electric current magnitude in the dayside region.

3. Observational Facts for Event on 16 July 2007

We consider the interval from 19:00 to 21:00 UT on 16 July 2007. Note that some of the observational facts important for our study were previously mentioned by *Jelínek et al.* [2010] and *Suvorova et al.* [2010]. Figure 1 shows the positions of THEMIS, Geotail, and GOES 11 projected onto the $z = -3 R_E$ GSM plane (THEMIS and GOES 11 were close to this plane). The THEMIS probes moved away from the Earth. THEMIS B (THB) is the outermost of the five THEMIS probes, and THEMIS A (THA) is the innermost. In addition to the previously published THEMIS and Geotail data, we also use GOES 11 data from nearly the same MLT sector.

Figures 2a–2d show the density and magnetic field observed by THEMIS A, B, and C. THB was in the magnetosphere before 19:00, entered into the magnetosheath for 5 min from 19:11 to 19:16 UT, then returned into the magnetosphere for 4 min, and at 19:20 moved into the magnetosheath again (magnetopause crossings are shown by vertical dashed lines in Figures 2a–2d). These and subsequent magnetopause crossings in observations were determined from both density and magnetic field variations; in particular the density was larger than 1 cm^{-3}, and B_z was negative or close to 0 in the magnetosheath.
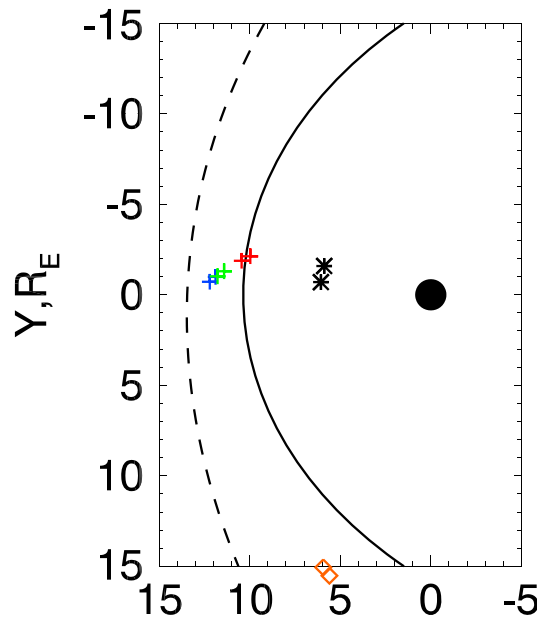
Figure 1. THB (blue), THC (green), and THA (red) positions in the subsolar magnetosheath/magnetopause region, GOES 11 (black) in the magnetosphere, and Geotail (orange) in the dusk magnetosheath projected on the $z = -3 R_E$ GSM plane at 20:00 and 20:30 UT on 16 July 2007. The model magnetopause [*Shue et al.*, 1998] and bow shock [*Formisano*, 1979] are shown for reference.

THB stayed in the magnetosheath until 19:58 UT. Then it observed a series of magnetopause crossings at 19:58, 20:11, 20:14, 20:21, 20:25, and 20:33 UT. Surprisingly, a few minutes later, at 20:37 and 20:39, THB registered a double bow shock crossing. This shows that the magnetosheath was about 70% thinner than usual, as discussed by *Jelínek et al.* [2010]. This is apparently a nonstationary feature related to fast magnetopause compression and earthward bow shock motion when the IMF becomes nonradial according to Wind data. After that, THB stayed in the magnetosheath.

As noted by *Suvorova et al.* [2010], the magnetopause positions were unusually distant between 19:58 and 20:33 UT. In this interval, the other THEMIS (THD, THC, and THE) spacecraft also moved from the magnetosheath to the magnetosphere as a consequence of magnetopause expansion, but THB observed the greatest magnetopause distance and we would like to reproduce it by a relevant model.

Figures 2e and 2f compare the IMF cone angles θ_{BX} observed by ACE and Wind with the magnetosheath (and magnetosphere) cone angles observed by THB, THC, and Geotail. The cone angle varies from 0° to 90°. The time lag to the subsolar magnetopause is 50 min for ACE and 53 min for Wind; the time lag between THEMIS and Geotail is 10 min. The time lag has been determined from the distance between spacecraft using average flow velocities. The time lag in the simulations below varies slightly with the solar wind velocity. Figure 2 shows that the cone angle decreases (i.e., the IMF becomes more radial) at nearly the same time in time-lagged ACE and Wind data, at ~19:26 UT. The cone angle increases at the end of the interval, shortly before 21:00 UT. However, Wind also observed an increase in the cone angle between 20:34 and 20:44 UT which was not observed by ACE. In this as well as in other events, ACE and Wind data differ in some details, particulary in cone angle variations, and therefore, we will use both ACE and Wind input conditions in the simulations below and compare the results.

As mentioned above, THB and THC were in the magnetosphere at 19:00 UT and crossed the magnetopause several times in the next 2 h interval. At the same time, Geotail stayed in the magnetosheath, except for a short magnetospheric passage between 20:40 and 20:42 UT. The time intervals of the THB magnetospheric passages are marked by shadow bars in Figure 2f. The cone angles from THB (THC) and other spacecraft can be consistent with each other only at those times when THB (THC) was in the magnetosheath.

Figures 2e and 2f show that the cone angles observed by both Geotail and THEMIS differ significantly from those in the solar wind data. Even more, the cone angles from Geotail and THEMIS (when the THEMIS spacecraft were in the magnetosheath) correlate poorly with each other. Only the THB and THC data correlate well most of the time because the distance between THB and THC does not exceed 4200 km in this interval.

The weak correlation between IMF orientations in the solar wind and magnetosheath is typical for radial IMF conditions. It is related both to foreshock fluctuations which modify the upstream magnetic field and to the magnetosheath flow diversion. Draping effects align magnetic field lines in the magnetosheath along the magnetopause; therefore, the cone angle near the subsolar point approaches 90°. Moreover, the correlation length in the solar wind transverse to the Sun-Earth line is smaller for radial IMF than for IMF directed perpendicular to the Sun-Earth line [e.g., *Crooker et al.*, 1982].

Figure 3 shows the solar wind dynamic pressure from ACE and Wind, and the magnetosheath (magnetosphere) total pressure (including the dynamic pressure) from THB, THC, and Geotail. There is a data gap in the ion
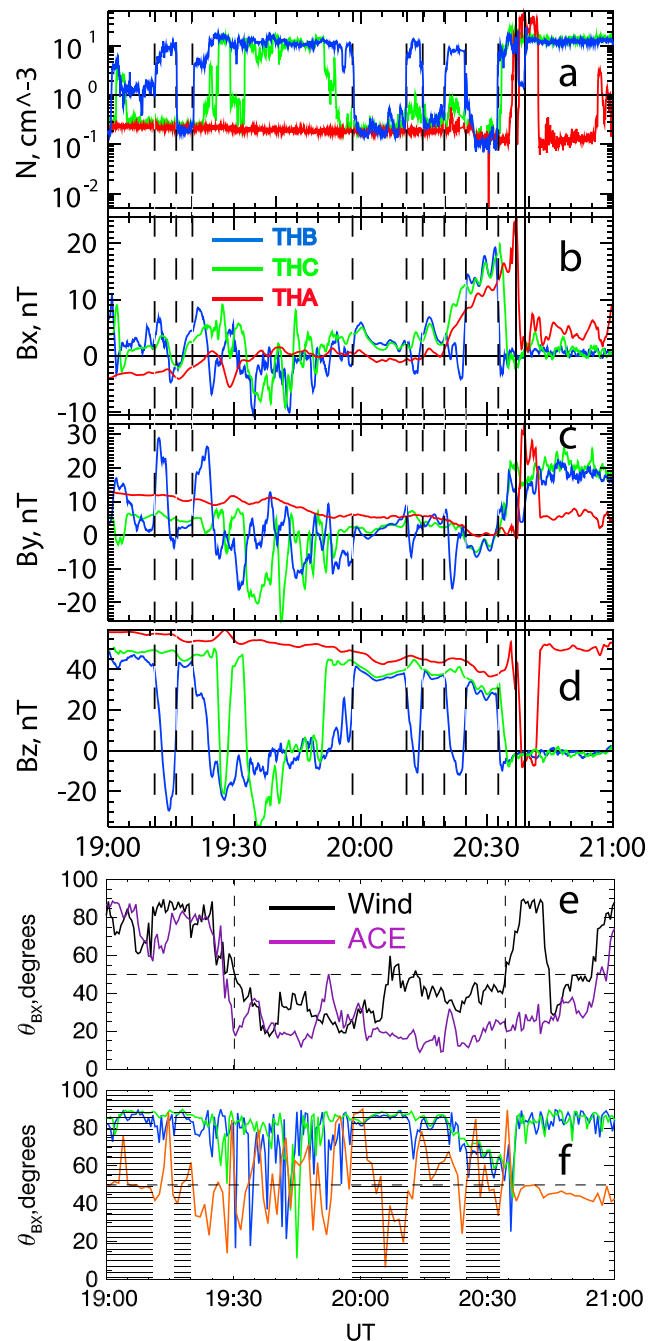
Figure 2. (a) Density and (b–d) magnetic field components observed by THA, THB, and THC for the event on 16 July 2007. Vertical dashed lines mark magnetopause crossings observed by THB; two vertical solid lines at 20:37 and 20:39 UT mark a THB double bow shock crossing. (e) The time-lagged IMF cone angles from Wind and ACE; (f) the cone angles from THB (blue), THC (green), and Geotail (orange). Horizontal dashed lines point out the $\theta_{BX} = 50°$ (the solar wind conditions in numerical modeling are modified for $\theta_{BX} < 50°$). Vertical dashed lines (Figure 2e) mark the quasi-radial interval (between 19:30 and 20:34 UT) in Wind data. Time intervals of THB magnetosphere passages (Figure 2f) are indicated by shadow bars.

velocity from THEMIS after 20:27 UT; therefore, we also show the sum of magnetic and thermal pressures which nearly coincides with the total pressure 95% of the time near the magnetopause.

At the beginning and end of the interval, at 19:00 and 21:00 UT, the solar wind pressure (ACE and Wind), the total pressure near the subsolar magnetopause (THEMIS at 19:00), and the total pressure in the flank magnetosheath (Geotail) are nearly equal at 1 nPa. This shows the agreement between the measurements from
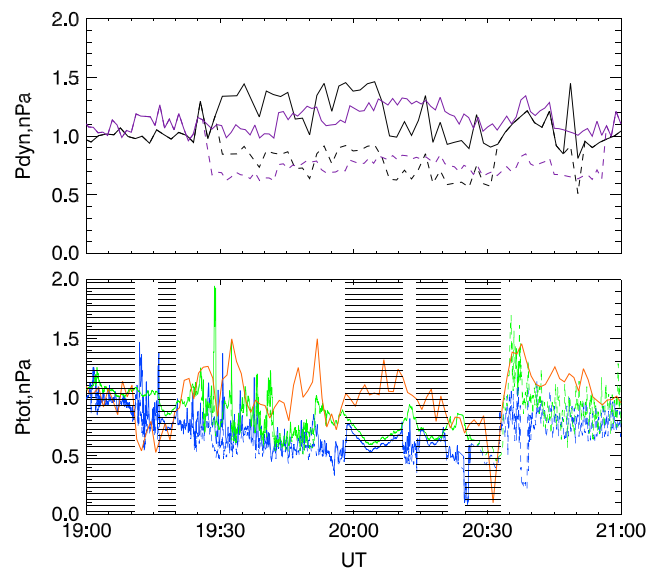
Figure 3. (top) The measured solar wind dynamic pressure from Wind (black, solid) and ACE (violet, solid), and the modified solar wind pressure reduced to 53% in the foreshock region as explained in section 3 (dashed lines). (bottom) The total pressure (the sum of magnetic, thermal, and dynamic pressures) from THB (blue), THC (green), and Geotail (orange). Dashed blue (green) lines show the sum of magnetic and thermal pressures from THB (THC). Time intervals of THB magnetosphere passages are indicated by shadow bars.

the four probes outside the radial IMF interval. The Wind and ACE dynamic pressures are on average about 1.16 nPa during the radial IMF interval, although both pressures exhibit significant changes. The Wind pressure is higher in the first half (until ∼20:07) of the radial interval, while the ACE pressure is higher in the second half of the interval.

The THB total pressure is highly variable but tends to decrease until 19:55 UT. During multiple magnetopause crossings between 19:58 and 20:33 UT, the average THB pressure is ∼0.59 nPa, i.e., about half the average solar wind pressure. THC, closer to the Earth, registers higher total pressures than THB during almost the whole interval. In general, the curve for the THC pressure tracks that for the THB pressure variations, but occasionally the difference between the pressures exceeds 0.4 nPa, e.g., at 19:55 UT. We expect that the magnetopause position can be very variable in such conditions.

Interestingly, the Geotail total pressure does not follow the decrease in THB pressure. Although the Geotail pressure is also highly variable, the average pressure in the 2 h interval is 1.06 nPa, i.e., ∼91% of the average solar wind pressure. This small decrease of the total pressure in the magnetosheath can be explained without taking into account the foreshock effect [*Samsonov et al.*, 2012].

Magnetic field measurements from GOES 11 in the dayside magnetosphere complete the observations of this event. GOES 11 was slightly dawnward from noon and below the equatorial plane like the five THEMIS probes (see Figure 1); therefore, GOES 11 should not miss the large magnetopause oscillations observed by THEMIS. Indeed, Figure 4 shows that GOES 11 observed a relatively small decrease in B_z at 19:30 when the time-lagged IMF becomes radial, while an increase in B_z at 20:34 indicates the end of the radial IMF interval according to the Wind data. Figure 4 also displays the results of global MHD simulations along GOES 11 trajectory in runs 2 and 3 (discussed below).

Let us emphasize some observational facts important for interpretation of the numerical results in the next section.

1. Both ACE and Wind observe quasi-radial IMF orientations nearly at the same time; however, there are a few important differences between the observations from both solar wind monitors, e.g., in the dynamic pressure and IMF cone angle variations. Below we compare the numerical results with both the ACE and Wind input conditions and find that the observed magnetopause crossings are better reproduced using the Wind data. We suppose that the strong magnetospheric compression manifested by the THB double bow shock crossing at 20:37 and 20:39 UT, the THA magnetopause crossings between 20:36 and 20:42 UT, and the GOES 11 B_z increase between 20:34 and 20:40 UT results from the transition from radial to nonradial IMF observed by Wind at 20:34 UT (in time-lagged data), while ACE detects the same transition only at 20:54 UT. This is also confirmed by *Jelínek et al.* [2010] who noted a dropout of energetic ions in THEMIS data at ∼20:36 UT suggesting that the upstream bow shock changed from quasi-parallel to quasi-perpendicular. Note that Wind is located farther from the Sun-Earth line and the difference between the ACE and Wind positions lies mainly in the y direction. The reason why Wind input conditions are better remains unclear. However, we can suggest the following explanation. The Wind position in GSE coordinates at 19:00 UT is (254, −67, 17) R_E, and the velocity measured by 3DP-PM on board Wind at this time is (−454, 34, 4) km/s. This means that the angle between the velocity vector and the Sun-Earth line in the equatorial GSE plane
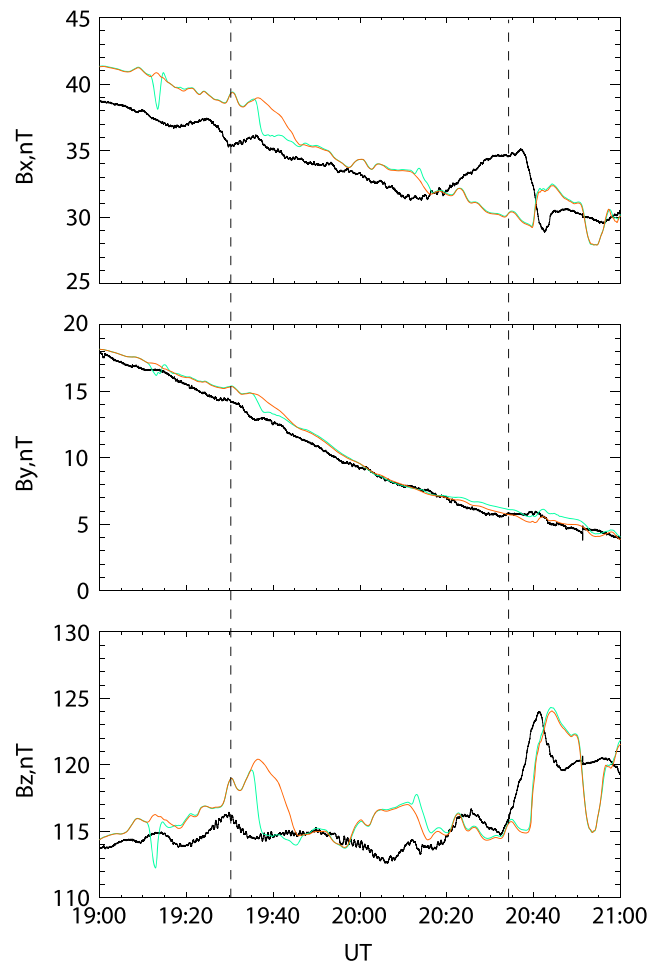
Figure 4. Magnetic field observed by GOES 11 (black) and obtained by the MHD simulation in runs 2 (green) and 3 (red). We add constant values to the simulated B_y (+5 nT) and B_z (+10 nT) components in order to get a better correspondence in the initial conditions. Vertical lines mark the radial IMF interval as observed by Wind (the same as in Figure 2d).

is 4.3°, and the angle between the Wind position and the Sun-Earth line is 14.8°. Although this does not prove that the simulations with Wind input conditions will give better results, it does demonstrate that the solar wind flow is not directed along the Sun-Earth line. The finite positive V_y measured by the 3DP-PM monitor shows that conditions at the nose of the magnetopause will be determined by solar wind structures coming from a location in between ACE and Wind (our estimation is at $y = -19\,R_E$). Comparison of ACE and Wind observations shows a very disturbed IMF, and thus it is not surprising that none of these upstream monitors could be used for an exact estimation of IMF orientation just in front of the bow shock.

2. The 50% total pressure decrease in the magnetosheath observed by THEMIS is a local, rather than a global, feature because the total pressure from Geotail (at $y = 15\,R_E$) is only slightly smaller than the solar wind dynamic pressure. GOES 11 at geosynchronous orbit in the dayside magnetosphere also may observe weaker changes of the magnetic field than expected from the pressure variations at THEMIS (see comparison with numerical results in next section).

4. Comparison Between Numerical Simulations and Spacecraft Observations

4.1. Event on 16 July 2007 (Solar Wind Dynamic Pressure ∼1.3 nPa)

In this event, we have made several simulation runs using different solar wind boundary conditions and below present only three of them for ACE and Wind. In run 1, we have used the initial Wind (or ACE) data with a time lag for solar wind propagation to the model inflow boundary. In run 2, we have changed the solar wind parameters during intervals when the cone angle $\theta_{BX} < 50°$. These changes include a density decrease to 60%, a V_X velocity decrease to 94%, and a temperature increase to 200%. This agrees with statistical results
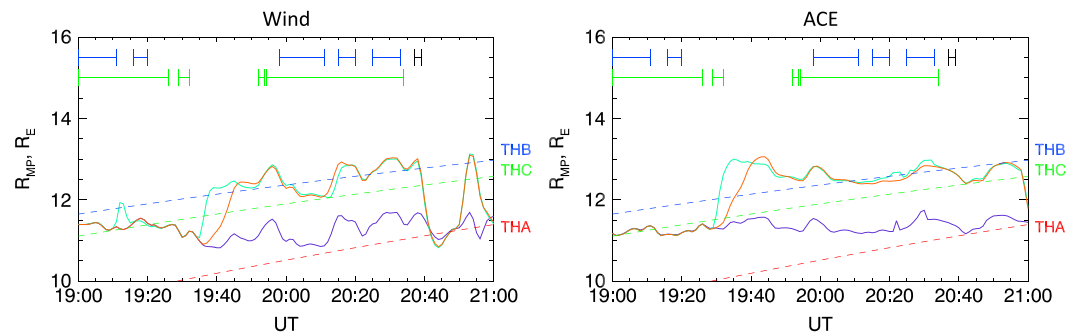
Figure 5. Magnetopause radial distance approximately along the line between the Earth and THEMIS in runs 1 (dark blue), 2 (green), and 3 (red) for the event on 16 July 2007 using (left) Wind and (right) ACE input solar wind conditions, and the radial distances to THA, THB, and THC. The upper bars mark the intervals when THB (blue) and THC (green) were in the magnetosphere. The black upper bar indicates the THB double bow shock crossing.

[*Billingham et al.*, 2008; *Cao et al.*, 2009; *Urbar et al.*, 2013]. Thus, the solar wind dynamic pressure is reduced by 53% during such intervals. We also have tried to reduce the IMF B_y and B_z to 60% in agreement with *Billingham et al.* [2008], but these changes have negligible effects on the results.

In run 3 (discussed in detail below), we have made the same changes as in run 2, but the transition from nonmodified to modified plasma parameters is extended over 10 min. We have simulated runs 1–3 using both Wind and ACE input conditions; accordingly, we present in total the results of six runs below.

We use the high threshold of $\theta_{BX} = 50°$ to exclude abrupt changes between modified and nonmodified solar wind parameters because the Wind θ_{BX} is highly variable and briefly exceeds 40–50° during the radial interval 19:30–20:34 UT. We have tried smaller thresholds for θ_{BX} and got negligible changes in the solution. Although the resolution of Wind data is 3 s, we use 1 min averages when determining θ_{BX}. In Figure 3, the artificially reduced solar wind pressures from ACE and Wind are shown by dashed lines.

The main purpose of the simulations is to reproduce the unusual magnetospheric expansion after 19:50 UT. Figure 5 shows the variations of the predicted magnetopause distance along the line between the Earth and the THEMIS spacecraft in runs 1, 2, and 3 (explained below). We also trace the radial distance to the THEMIS spacecraft by dashed lines. A spacecraft stays in the model magnetosphere if its radial distance lies below the magnetopause position and in the magnetosheath otherwise. For comparison, two upper color bars mark the intervals when THB (blue) and THC (green) were in the magnetosphere according to the observations. Figure 5 (left and right) corresponds to the simulations with Wind and ACE solar wind conditions. Below we discuss the runs with the Wind input conditions which, in our opinion, better reproduce the observed magnetospheric expansion.

In run 1, the artificial THB stays in the magnetosheath throughout the whole 2 h interval, and THC remains in the magnetosphere only until 19:20 UT and then moves into the magnetosheath, too. Thus, the model fails to predict the observed magnetopause crossings after 19:50 UT.

The decreases of the density and V_X in run 2 obviously result in an outward magnetopause displacement. The magnetopause position shifts outward by ~1.3 R_E on average. In this case, the artificial THC returns to the magnetosphere at 19:36 and remains there until 20:39 UT. Thus, the modified simulation overestimates the magnetopause distance, because the real THC was in the magnetosphere only between 19:52 and 20:34 UT. Similarly, the artificial THB stays in the magnetosphere longer than the real one. There are some discrepancies, e.g., between 20:01 and 20:15 UT when the artificial THB is in the magnetosheath, while the real THB is in the magnetosphere until 20:11 UT, and then in the magnetosheath until 20:15 UT, again crossing the magnetopause exactly at the same time as predicted by the model.

Using simple time-lagged solar wind data, we estimate that the IMF observed both by ACE and Wind becomes quasi-radial at the subsolar magnetopause at ~19:30 UT, while the THEMIS spacecraft observe the series of magnetopause crossings related to the radial IMF only from ~19:51 UT. We attempted to determine the orientation of the directional discontinuity at ~18:32 UT in Wind (non-time-lagged) data, and our analysis shows that the normal to this discontinuity lay nearly in the *z* direction with only a small *x* component, while $V_Z \simeq 0$. It is difficult to determine when this discontinuity reached the subsolar point. It is possible that the time

lag for this discontinuity is about 75 min, which would give an arrival time at the subsolar point of ∼19:47 UT in rather good agreement with the THEMIS observations. However, we cannot take into account this factor in the model because this estimation is not precise and the time lag may change significantly during the interval.

We suggest another possible explanation for the time delay. Suppose the radial turning of the IMF reaches the subsolar bow shock at ∼19:30 UT but the changes of the solar wind density and velocity in the foreshock develop very gradually (linearly varying from the beginning to final values). We verify this assumption in run 3. In this run, the density, V_X, and temperature vary in the same manner as in run 2, but the transformation from the nonradial to radial state broadens to last 10 min. Results from run 3 in Figure 5 significantly differ from the results of run 2 only between 19:35 and 19:46 UT giving about a 10 min delay of the outward magnetopause motion. The numerical results still differ from the observations because THB observed the magnetopause crossing only at 19:58 UT; however, the prediction of the last run approaches closer to the observations.

A third alternative explanation of the time delay may be obtained by comparing GOES 11 data with the simulation results in Figure 4. The magnitude of the B_z increase at 20:34 UT in GOES 11 data coincides well with the model predictions in runs 2 and 3. But the observed decrease in B_z at 19:30 UT is only 2 nT, while the model predicts a decrease by 5 nT at 19:35 UT (in run 2) when the pressure reduction is applied. However, the second observed B_z decrease by ∼2 nT occurs between 19:54 and 20:06 UT. Therefore, we surmise that the cone angle, and correspondingly the total pressure upstream from the subsolar bow shock, changes in two steps which correspond to the two B_z decreases. This assumption does not contradict the sequence of magnetopause crossings observed by THEMIS between 19:51 and 20:34 UT.

The THEMIS observations actually agree with this idea of several steps decrease of the total pressure in the magnetosheath. Figure 6 compares the total pressure observed by THEMIS (also shown in Figure 3 above) with simulation results from runs 1–3. The total pressure in run 1 significantly exceeds the pressure observed by THB during the radial IMF interval. After the magnetopause crossing at 19:20 UT, the THB pressure initially drops at 19:28 UT, i.e., even before the predicted pressure decrease at ∼19:35 UT. However, the decrease of the observed THB pressure is followed by an increase from 19:30 to 19:36, then a second decrease from 19:36 to 19:41 UT, and a third decrease at ∼19:55 UT. It seems that the last moderately small pressure decrease also observed in the Wind input data and the MHD simulations is related to outward magnetopause motion at THB (19:58 UT). The THB and THC total pressures abruptly increase at these magnetopause crossings (at 19:52 UT in THC data) indicating that the magnetopause is not in pressure balance. Inside the magnetosphere, the observed pressure is usually higher than the simulated one (in runs 2 and 3) but also shows some variations which are not predictable from upstream solar wind conditions and seem to be local spatial structures.

There is a data gap in the THEMIS velocity measurements after 20:27 UT, but the magnetic and thermal pressures are still available, and we calculate their sum. The contribution of the dynamic pressure to the total pressure near the subsolar magnetopause is usually negligible. The fast inward magnetopause motion at 20:33 (THB) and 20:34 UT (THC) is followed by a sharp pressure increase observed in the magnetosheath at ∼20:34 UT by both THB and THC and then even by the double bow shock crossings in THB data (20:37–20:39 UT). These impressive changes result solely from variations of the IMF cone angle because of which the bow shock is transformed from quasi-parallel to quasi-perpendicular near noon.

Checking our assumption about the density decrease during the radial IMF interval, we have compared the simulated and observed density profiles along the THB and THC trajectory (not shown). Both THB and THC were in the magnetosheath between 19:40 and 19:50 UT. The average density in this interval observed by THB is only 70% of the simulated one in run 1 (without density changes); the average observed density from THC is 76% of the simulated one, while between 19:30 and 19:35 the observed and simulated densities nearly coincide. The simulated density in runs 2 and 3 is less than that observed during this time interval because the artificial spacecraft are in the magnetosphere. This strongly indicates that the pristine solar wind density observed by Wind was larger than that affecting the bow shock and should be decreased (at least to 70–76%) for better agreement with the THEMIS data in the magnetosheath. Moreover, the decrease of density from THB at 19:40 may indicate the time when the foreshock structure with reduced dynamic pressure was formed.

4.2. Event on 22 July 2007 (Solar Wind Dynamic Pressure 1.1 nPa)

In this and the two following events, THEMIS was also located in the subsolar region and observed distant magnetopause crossings and weaker total pressure than the upstream solar wind monitors. We have calculated the angle between the radius vector to THEMIS position and the IMF vector (using corresponding solar
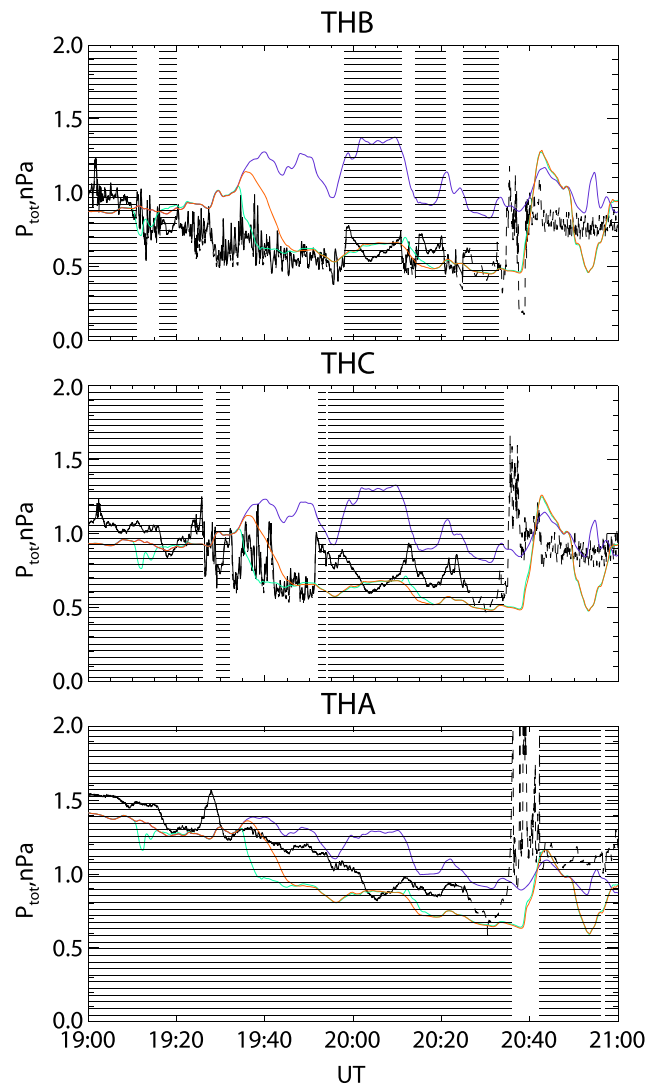
Figure 6. Total (magnetic, thermal, and dynamic) pressures from THEMIS (black), in runs 1 (dark blue), 2 (green), and 3 (red) for the event on 16 July 2007. Dashed black line shows the sum of magnetic and thermal pressures in THEMIS data. Shading indicates THEMIS magnetospheric intervals.

wind monitor) and found average values of these angles in every event. According to our rough estimations, the average angles were between 11° and 55°. Thus, THEMIS was mainly downstream of the quasi-parallel bow shock but occasionally downstream of the oblique shock. However, the IMF cone angle was below 45° during most of the time.

On 22 July 2007, the ACE and Wind observed that cone angles θ_{BX} generally remained below 50° but exceeded the threshold during several 1–10 min intervals. The average θ_{BX} was $\sim 40°$ between 12 and 17 UT. Although the cone angle was not very small, THEMIS observed multiple magnetopause crossings after 14:21 UT at radial distance $R_{MP} \geq 13\ R_E$, i.e., larger than MHD or empirical models predict for the given solar wind pressure (~ 0.9 nPa). We have simulated the magnetosphere with both the original and modified solar wind conditions obtained from both the ACE and Wind monitors. As in the previous case, the observed magnetopause crossings are better reproduced using Wind observations. Figure 7 compares the predicted magnetopause distance for run 1 (original Wind data) and run 2 (modified Wind data) with observed magnetopause crossings. The model cannot reproduce the distant magnetopause crossings without modification of the input conditions. But the reduction of solar wind density to 60% and V_x to 94% of the original data for $\theta_{BX} < 50°$ (the same as in the first case) allows us to predict the first magnetopause crossings nearly at the same time as those observed by THB and THD.

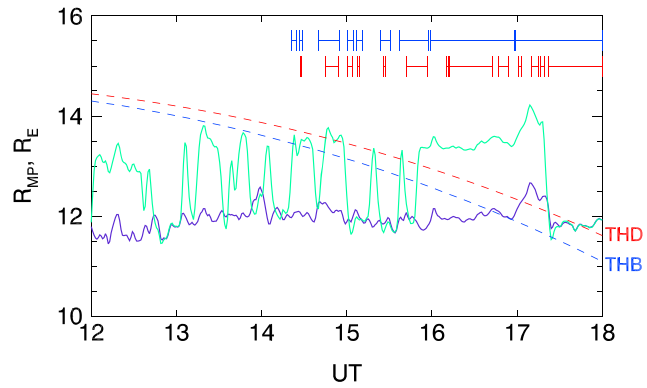**Figure 7.** Magnetopause radial distance for the event on 22 July 2007. The format is the same as in Figure 5.
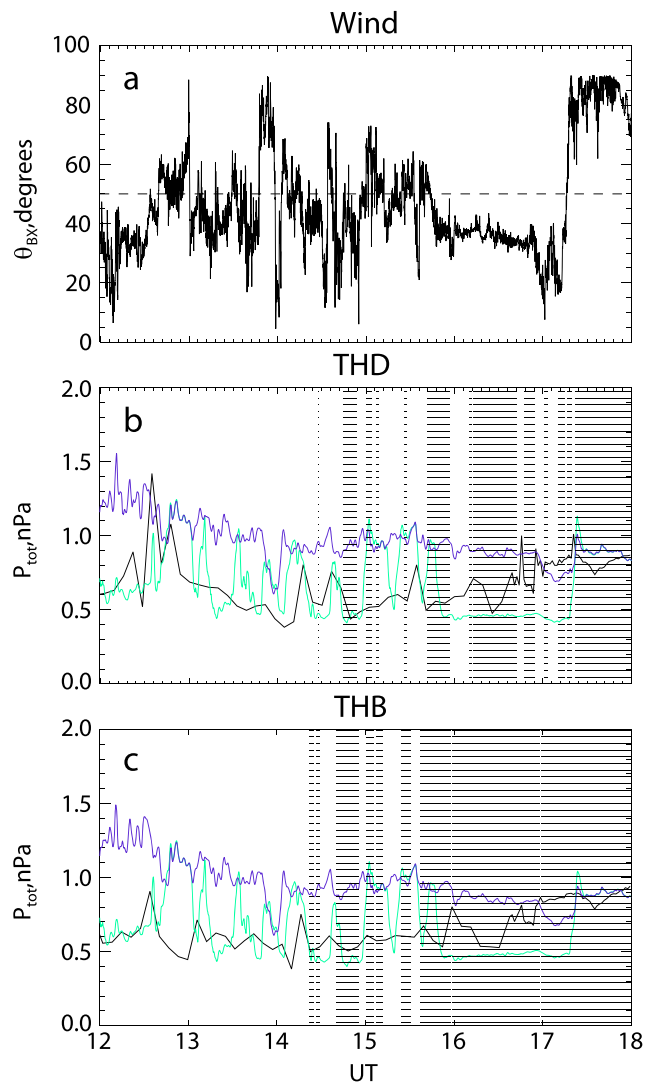

Figure 8. (a) IMF cone angle from the solar wind monitor whose data have been used for boundary conditions (see explanations in text). (b and c) Total pressure in THEMIS data (black line) and simulation runs 1 (dark blue) and 2 (green) for the event on 22 July 2007. Shading indicates THEMIS magnetospheric intervals.
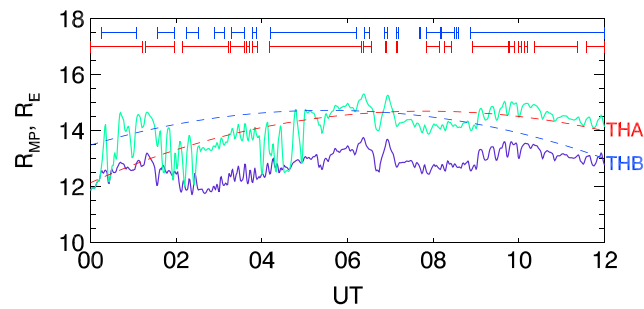
Figure 9. Magnetopause radial distance for the event on 13 July 2007. The format is the same as in Figure 5.

As mentioned above, the cone angle θ_{BX} at Wind exceeds the 50° threshold several times during the interval. As a result, the modified solar wind dynamic pressure in run 2 abruptly increases and decreases several times resulting in inward and outward magnetopause motion predicted in the simulation. We believe that the multiple magnetopause crossings observed by THEMIS result from local variations in the foreshock and are not related to solar wind parameters at L1; therefore, we do not expect that simulated and observed magnetopause crossings will correlate well during the radial IMF interval. The input θ_{BX} and correspondingly modified dynamic pressure abruptly increase at ∼17:20 UT causing the magnetospheric compression in run 2, and the results of both runs coincide at the end of the interval. THEMIS was approaching the Earth at a radial distance of ∼12 R_E at this time, and the simulation results for the original solar wind conditions (run 1) reasonably well reproduce the observed magnetopause positions.

Figure 8 compares the total pressure in runs 1 and 2 with the THEMIS data. The simulated total pressure in run 2 varies greatly in response to variations of θ_{BX}. The observed total pressure lies close to the lower threshold of the simulated pressure until ∼16 UT but also exhibits large variations. After 16 UT, the THEMIS spacecraft remain mostly in the magnetosphere and the observed total pressure lies between those predicted by runs 1 and 2.

4.3. Event on 13 July 2007 (Solar Wind Dynamic Pressure 0.8 nPa)

THEMIS observed multiple magnetopause crossings throughout the whole 12 h interval on 13 July 2007 when θ_{BX} at Wind varied around 40°, while θ_{BX} at ACE remained mainly between 10° and 20°. Figure 9 shows predicted and observed magnetopause positions for this event. We use Wind input conditions because in that case the simulations match THEMIS observations slightly better. The THEMIS spacecraft reached apogees between 06 and 08 UT at $R \simeq 14.7\ R_E$. Wind observed the solar wind pressures that varied between 0.4 and 0.9 nPa, which is lower than normal but still not small enough to explain such distant magnetopause crossings.

The MHD model with the observed solar wind pressure (run 1) predicts only a few THA magnetopause crossings during the first hour of the interval. The magnetopause distance R_{MP} in run 2 (with decreased solar wind pressure) roughly follows the THA trajectory in particularly increasing from 02 to 06 UT. However, the predicted R_{MP} is still slightly underestimated because the artificial THB stays longer in the magnetosheath than the real spacecraft. Since the radial distance between THA and THB sometimes exceeds 1 R_E, while both spacecraft observe almost simultaneous magnetopause crossings, we conclude that the amplitude of the magnetopause oscillations is large.

Figure 10 shows the simulated and observed total pressure for this event. During the first half of the interval, the total pressure in run 2 lies close to the THEMIS observations. During the second half, the observed pressure is sometimes higher than the simulated one, but the difference is smaller for THA which is the outermost spacecraft at this time. In general, the observations confirm our assumption about the pressure correction in this case.

4.4. Event on 4 August 2007 (Solar Wind Dynamic Pressure 0.6 nPa)

For simulations of the 18 h interval on 4 August, we have used ACE solar wind observations. The angle θ_{BX} at ACE lies below 20° most of the time from 02 to 12 UT and then increases to remain mostly above 45° after 15 UT. Figure 11 shows the magnetopause positions. The challenge in this case is to predict magnetopause crossings near apogee, between 09 and 12 UT. And the simulation with modified input conditions does predict $R_{MP} \simeq 14.7\ R_E$ close to the THEMIS trajectories. After 13 UT, the THEMIS spacecraft moved toward the Earth, while θ_{BX} increased. The run 2 simulation overestimates the magnetopause distance at this time; however, it
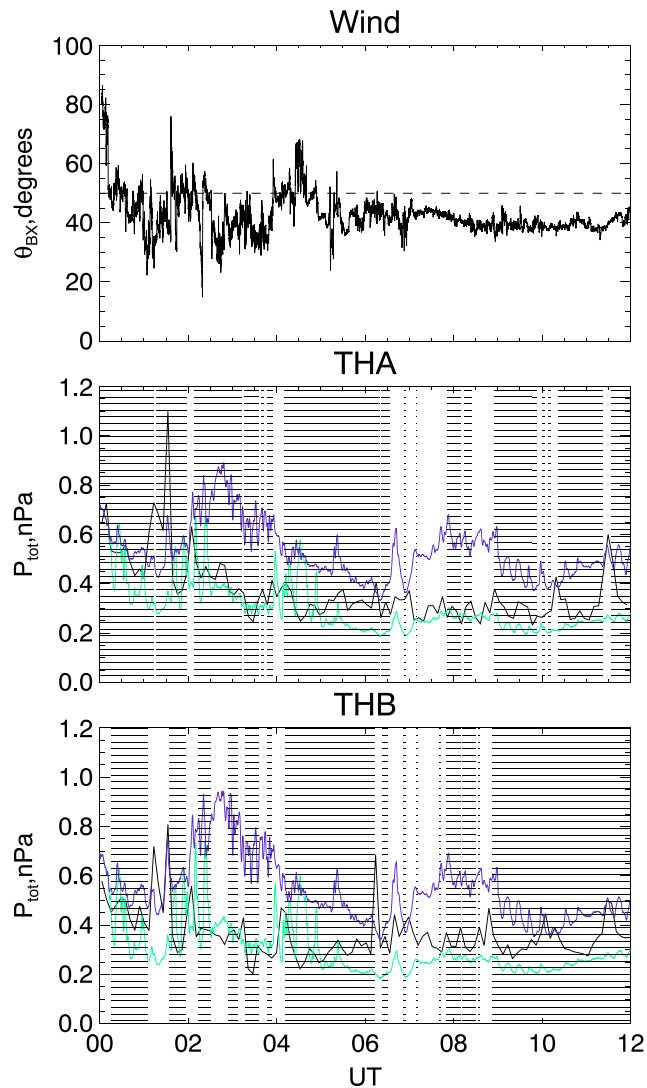
Figure 10. IMF cone angle from Wind and total pressure in THEMIS data and simulations for the event on 13 July 2007. The format is the same as in Figure 8.

is possible that the bow shock already became quasi-perpendicular because θ_{BX} was greater than 45° at Wind between 12 and 16 UT.

Figure 12 shows the total pressure. Although all the THEMIS spacecraft were rather deep in the magnetosphere at the beginning, THB observed short magnetosheath passages at 02:39, 04:08, 04:31, and 05:24 UT. The IMF θ_{BX} was already small; therefore, large-amplitude magnetopause oscillations (related also to the
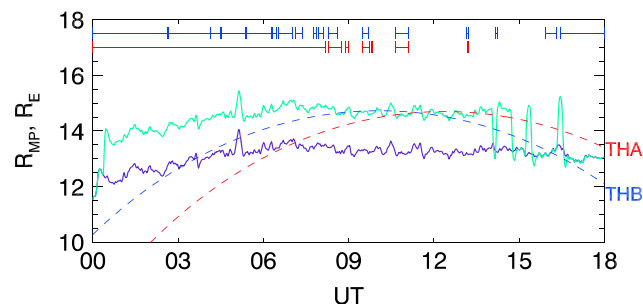

Figure 11. Magnetopause radial distance for the event on 4 August 2007. The format is the same as in Figure 5.
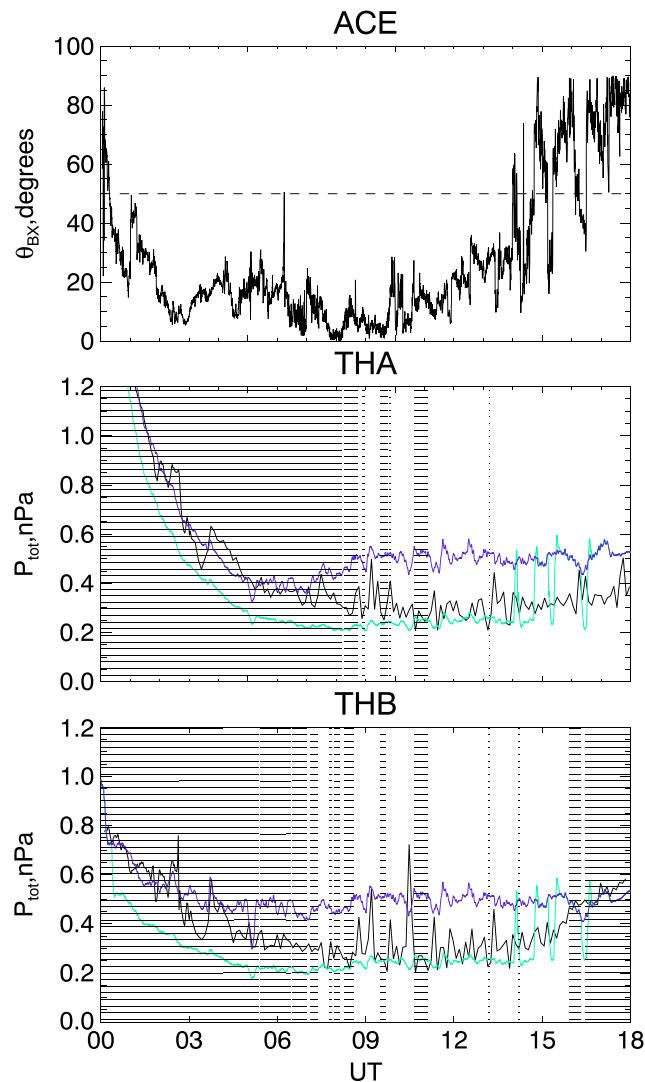
Figure 12. IMF cone angle from ACE (used as a solar wind monitor in this case) and total pressure in THEMIS data and simulations for the event on 4 August 2007. The format is the same as in Figure 8.

observed pressure variations at THA and THB) may occur. Although the run 1 simulation does not predict the magnetopause crossings well (see Figure 11), the total pressure at THA (and, to a lesser degree, the pressure from THB farther out) is better reproduced by run 1 than by run 2 from 00 to 05 (THB) and to 07 (THA) UT. Thus, the pressure decrease initiated in the foreshock changes the average pressure in the magnetosheath but may not influence the average pressure in the magnetosphere very much. However, pressure variations (compressional waves) can easily penetrate into the magnetosphere, as is evident at the beginning of this event (see large variations of the total pressure from THA and THB between 02 and 05 UT in Figure 12). The observed total pressure is close to the simulated one in run 2 between 08 and 15 UT for THB and between 10 and 15 UT for THA. The total pressure increases at the end of the interval with increase of θ_{BX}.

5. Conclusions

In this paper, we suggested a method for incorporating kinetic foreshock effects into a global MHD model by modifying the solar wind boundary conditions. We selected four events observed by THEMIS in 2007 that were characterized by large magnetospheric expansions during which the IMF cone angle θ_{BX} remained small. We simulated these events with the SWMF (former BATS-R-US) global isotropic MHD model. We took into account results from statistical analysis that provided quantitative estimations of the density and velocity reductions in the foreshock upstream of the bow shock [*Billingham et al.*, 2008; *Cao et al.*, 2009;

Urbar et al., 2013]. Besides, *Cao et al.* [2009] noted thermalization of solar wind ions. We artificially changed the solar wind boundary conditions in the numerical model for the intervals when the IMF cone angle decreased below 50°. In particular, we decreased the density by 40% and the velocity by 6% and increased the temperature by 100%, thereby reducing the solar wind dynamic pressure upstream from the bow shock to 53% of the observed dynamic pressure near L1.

We find that the global MHD model with these changes in the solar wind conditions predicts magnetospheric expansions with nearly the same magnitude as those observed by the THEMIS spacecraft. The magnetopause position shifts on average by $1.3-1.5\,R_E$ outward during these events. This agrees well with the statistical results of *Dušík et al.* [2010] who obtained the difference in magnetopause positions for $\theta_{BX}=0°$ and 180° from $\theta_{BX}\simeq 90°$ at $\sim 1.4\,R_E$. On the contrary, simulations with unmodified solar wind conditions do not predict the magnetospheric expansion in response to the θ_{BX} decrease and therefore cannot reproduce the observed magnetopause crossings.

We compared the simulated and observed total pressures in the magnetosheath and magnetosphere. Most of the time, the total pressure in the runs with modified solar wind conditions agreed better with observations in the magnetosheath. However, the total pressure at THEMIS occasionally (and mostly in the magnetosphere) came close to the numerical results with original (unchanged) input conditions.

Predicting the magnetopause response during radial IMF intervals can be difficult because solar wind monitors near L1 may observe local structures which do not affect the magnetosphere or miss some structures which do pass through the subsolar region. Furthermore, even with perfect solar wind observations and magnetospheric models it will not be possible to predict every magnetopause crossing because large pressure oscillations appear stochastically in the foreshock.

We realize that the pressure decrease in the foreshock is a large-scale but spatially localized structure, with a typical size of up to tens of Earth radii as shown by *Omidi et al.* [2010], while we have changed the MHD boundary conditions globally through the whole inflow solar wind boundary. Therefore, the method we suggest is not perfect and allows us to reproduce correctly only the portion of the magnetopause behind the foreshock, and not even all of that, since prolonged magnetic connection to the bow shock is required to generate the depressed dynamic pressures that allow the magnetopause to move outward. The actual size of the expanded area will depend on the IMF orientation. It could be a large part of the dayside region for a radial IMF or just dawnside for a spiral IMF. For example, in the event on 16 July 2007, Geotail at $y = 15\,R_E$ (still on the dayside) did not observe the pressure decrease as THEMIS did in the subsolar magnetosheath.

Possibly a more correct approach would be to change the boundary conditions locally in the foreshock while keeping unchanged solar wind parameters throughout the remainder of the solar wind boundary, but this would require significant modifications to existing numerical codes. Alternatively, our method could be confirmed by statistical analysis of a large number of magnetopause crossings. However, such study is very difficult because results also depend on the y and z components of the solar wind flow velocity. These components often result from Alfvenic waves that propagate in the solar wind frame, making the precise timing of distant monitors difficult.

We decreased the solar wind dynamic pressure for small θ_{BX} intervals mainly by reducing the density and assuming only small changes of the V_x. However, variations of the plasma parameters in the foreshock are still not well understood and they may at times consist of a large decrease or deflection of the flow velocity from the Sun-Earth line together with relatively small changes or even an increase of density. To study this possibility, we simulated a case in which the modified V_x fell to 53% of its original value, but the density increased to 188.6% of the original values. These changes keep the flux (density multiplied by V_x) constant. The calculated R_{MP} in this case (not shown) exhibits large overshoots at the beginning and end of radial IMF intervals (with amplitudes of several R_E), but in the middle of the interval the R_{MP} remains close to the previously calculated locations. More accurate estimations of average plasma parameters in the foreshock hopefully will be obtained in future studies from in situ observations and statistical analysis.

In this work, we use only the isotropic global MHD model, and the explanation for the pressure decrease for radial IMF suggested here differs from that of *Samsonov et al.* [2012]. Our assumptions permit us to obtain a greater pressure reduction near the magnetopause than that predicted by *Samsonov et al.* [2012] in the anisotropic MHD simulations without the foreshock effects. However, the total pressure reductions in the foreshock and through the magnetosheath do not contradict each other. Both effects are important in numerical modeling and can be combined in future.

References

Archer, M. O., D. L. Turner, J. P. Eastwood, S. J. Schwartz, and T. S. Horbury (2015), Global impacts of a foreshock bubble: Magnetosheath, magnetopause and ground-based observations, *Planet. Space Sci.*, *106*, 56–66, doi:10.1016/j.pss.2014.11.026.

Asbridge, J. R., S. J. Bame, and I. B. Strong (1968), Outward flow of protons from the Earth's bow shock, *J. Geophys. Res.*, *73*(17), 5777–5782, doi:10.1029/JA073i017p05777.

Auster, H. U., et al. (2008), The THEMIS fluxgate magnetometer, *Space Sci. Rev.*, *141*, 235–264, doi:10.1007/s11214-008-9365-9.

Billingham, L., S. J. Schwartz, and D. G. Sibeck (2008), The statistics of foreshock cavities: Results of a Cluster survey, *Ann. Geophys.*, *26*, 3653–3667, doi:10.5194/angeo-26-3653-2008.

Cao, J. B., H. S. Fu, T. L. Zhang, H. Reme, I. Dandouras, and E. Lucek (2009), Direct evidence of solar wind deceleration in the foreshock of the Earth, *J. Geophys. Res.*, *114*, A02207, doi:10.1029/2008JA013524.

Crooker, N. U., G. L. Siscoe, C. T. Russell, and E. J. Smith (1982), Factors controlling degree of correlation between ISEE 1 and ISEE 3 interplanetary magnetic field measurements, *J. Geophys. Res.*, *87*(A4), 2224–2230, doi:10.1029/JA087iA04p02224.

Dušík, Š., G. Granko, J. Šafránková, Z. Němeček, and K. Jelínek (2010), IMF cone angle control of the magnetopause location: Statistical study, *Geophys. Res. Lett.*, *371*, L19103, doi:10.1029/2010GL044965.

Engebretson, M. J., L. J. Zanetti, T. A. Potemra, W. Baumjohann, H. Lühr, and M. H. Acuna (1987), Simultaneous observation of Pc 3–4 pulsations in the solar wind and in the Earth's magnetosphere, *J. Geophys. Res.*, *92*(A9), 10,053–10,062, doi:10.1029/JA092iA09p10053.

Fairfield, D. H., W. Baumjohann, G. Paschmann, H. Lühr, and D. G. Sibeck (1990), Upstream pressure variations associated with the bow shock and their effects on the magnetosphere, *J. Geophys. Res.*, *95*(A4), 3773–3786, doi:10.1029/JA095iA04p03773.

Formisano, V. (1979), Orientation and shape of the Earth's bow shock in three dimensions, *Planet. Space Sci.*, *27*(9), 1151–1161, doi:10.1016/0032-0633(79)90135-1.

Frank, L. A., K. L. Ackerson, W. R. Paterson, J. A. Lee, M. R. English, and G. L. Pickett (1994), The comprehensive plasma instrumentation (CPI) for the Geotail spacecraft, *J. Geomag. Geoelectr.*, *46*, 23–37.

Greenstadt, E. W., I. M. Green, G. T. Inouye, A. J. Hundhausen, S. J. Bame, and I. B. Strong (1968), Correlated magnetic field and plasma observations of the Earth's bow shock, *J. Geophys. Res.*, *73*(1), 51–60, doi:10.1029/JA073i001p00051.

Jelínek, K., Z. Němeček, J. Šafránková, J.-H. Shue, A. V. Suvorova, and D. G. Sibeck (2010), Thin magnetosheath as a consequence of the magnetopause deformation: THEMIS observations, *J. Geophys. Res.*, *115*, A10203, doi:10.1029/2010JA015345.

Karimabadi, H., et al. (2014), The link between shocks, turbulence, and magnetic reconnection in collisionless plasmas, *Phys. Plasmas*, *21*, 062308, doi:10.1063/1.4882875.

Kokubun, S., T. Yamamoto, M. H. Acuna, K. Hayashi, K. Shiokawa, and H. Kawano (1994), The Geotail magnetic field experiment, *J. Geomag. Geoelectr.*, *46*, 7–21.

Kuznetsov, S. N., and A. V. Suvorova (1998), An empirical model of the magnetopause for broad ranges of solar wind pressure and B_z IMF, in *Polar Cap Boundary Phenomena*, edited by J. Moen, A. Egeland, and M. Lockwood, pp. 51–61, Kluwer Acad., Norwell, Mass.

Lepping, R. P., et al. (1995), The wind magnetic field investigation, *Space Sci. Rev.*, *71*, 207–229, doi:10.1007/BF00751330.

Lin, R. L., X. X. Zhang, S. Q. Liu, Y. L. Wang, and J. C. Gong (2010), A three-dimensional asymmetric magnetopause model, *J. Geophys. Res.*, *115*, A04207, doi:10.1029/2009JA014235.

McComas, D. J., S. J. Bame, P. Barker, W. C. Feldman, J. L. Phillips, P. Riley, and J. W. Griffee (1998), Solar Wind Electron Proton Alpha Monitor (SWEPAM) for the Advanced Composition Explorer, *Space Sci. Rev.*, *86*, 563–612, doi:10.1023/A:1005040232597.

McFadden, J. P., C. W. Carlson, D. Larson, M. Ludlam, R. Abiad, B. Elliott, P. Turin, M. Marckwordt, and V. Angelopoulos (2008), The THEMIS ESA plasma instrument and in-flight calibration, *Space Sci. Rev.*, *141*, 277–302, doi:10.1007/s11214-008-9440-2.

Merka, J., A. Szabo, J. Šafránková, and Z. Němeček (2003), Earth's bow shock and magnetopause in the case of a field-aligned upstream flow: Observation and model comparison, *J. Geophys. Res.*, *108*(A7), 1269, doi:10.1029/2002JA009697.

Ogilvie, K. W., et al. (1995), SWE, a comprehensive plasma instrument for the WIND spacecraft, *Space Sci. Rev.*, *71*, 55–77, doi:10.1007/BF00751326.

Omidi, N., J. P. Eastwood, and D. G. Sibeck (2010), Foreshock bubbles and their global magnetospheric impacts, *J. Geophys. Res.*, *115*, A06204, doi:10.1029/2009JA014828.

Palmroth, M., et al. (2015), ULF foreshock under radial IMF: THEMIS observations and global kinetic simulation Vlasiator results compared, *J. Geophys. Res. Space Physics*, *120*, 8782–8798, doi:10.1002/2015JA021526.

Park, J.-S., J.-H. Shue, K.-H. Kim, G. Pi, Z. Němeček, and J. Šafránková (2016), Global expansion of the dayside magnetopause for long-duration radial IMF events: Statistical study on GOES observations, *J. Geophys. Res. Space Physics*, *121*, 6480–6492, doi:10.1002/2016JA022772.

Paschmann, G., N. Sckopke, S. J. Bame, J. R. Asbridge, J. T. Gosling, C. T. Russell, and E. W. Greenstadt (1979), Association of low-frequency waves with suprathermal ions in the upstream solar wind, *Geophys. Res. Lett.*, *6*, 209–212, doi:10.1029/GL006i003p00209.

Pi, G., J.-H. Shue, J.-K. Chao, J. Němeček, Z. Šafránková, and C.-H. Lin (2014), A reexamination of long-duration radial IMF events, *J. Geophys. Res.*, *119*, 7005–7011, doi:10.1002/2014JA019993.

Pudovkin, M. I., B. P. Besser, and S. A. Zaitseva (1998), Magnetopause stand-off distance in dependence on the magnetosheath and solar wind parameters, *Ann. Geophys.*, *16*, 388–396.

Samsonov, A. A., Z. Němeček, J. Šafránková, and K. Jelínek (2012), Why does the subsolar magnetopause move sunward for radial interplanetary magnetic field?, *J. Geophys. Res.*, *117*, A05221, doi:10.1029/2011JA017429.

Samsonov, A. A., et al. (2016), Do we know the actual magnetopause position for typical solar wind conditions?, *J. Geophys. Res. Space Physics*, *121*, 6493–6508, doi:10.1002/2016JA022471.

Shue, J.-H., et al. (1998), Magnetopause location under extreme solar wind conditions, *J. Geophys. Res.*, *103*, 17,691–17,700, doi:10.1029/98JA01103.

Shue, J.-H., J.-K. Chao, P. Song, J. P. McFadden, A. Suvorova, V. Angelopoulos, K. H. Glassmeier, and F. Plaschke (2009), Anomalous magnetosheath flows and distorted subsolar magnetopause for radial interplanetary magnetic fields, *Geophys. Res. Lett.*, *36*, L18112, doi:10.1029/2009GL039842.

Sibeck, D. G., R. B. Decker, D. G. Mitchell, A. J. Lazarus, R. P. Lepping, and A. Szabo (2001), Solar wind preconditioning in the flank foreshock: IMP 8 observations, *J. Geophys. Res.*, *106*, 21,675–21,688, doi:10.1029/2000JA000417.

Smith, C. W., J. L'Heureux, N. F. Ness, M. H. Acuna, L. F. Burlaga, and J. Scheifele (1998), The ACE magnetic field experiment, *Space Sci. Rev.*, *86*, 613–632, doi:10.1023/A:1005092216668.

Suvorova, A. V., A. V. Dmitriev, and S. N. Kuznetsov (1999), Dayside magnetopause models, *Radiat. Meas.*, *30*, 687–692, doi:10.1016/S1350-4487(99)00220-6.

Suvorova, A. V., and A. V. Dmitriev (2015), Magnetopause inflation under radial IMF: Comparison of models, *Earth Space Sci.*, *2*, 107–114, doi:10.1002/2014EA000084.

Suvorova, A. V., et al. (2010), Magnetopause expansion for quasi-radial interplanetary magnetic field: THEMIS and Geotail observations, *J. Geophys. Res.*, *115*, A10216, doi:10.1029/2010JA015404.

Tóth, G., et al. (2005), Space Weather Modeling Framework: A new tool for the space science community, *J. Geophys. Res.*, *110*, A12226, doi:10.1029/2005JA011126.

Tóth, G., et al. (2012), Adaptive numerical algorithms in space weather modeling, *J. Comput. Phys.*, *231*, 870–903, doi:10.1016/j.jcp.2011.02.006.

Turner, D. L., N. Omidi, D. G. Sibeck, and V. Angelopoulos (2013), First observations of foreshock bubbles upstream of Earth's bow shock: Characteristics and comparisons to HFAs, *J. Geophys. Res. Space Physics*, *118*, 1552–1570, doi:10.1002/jgra.50198.

Troitskaya, V. A., T. A. Plyasova-Bakunina, and A. V. Gul'elmi (1971), The connection of Pc2–4 pulsations, *Doklady Akademiia Nauk SSSR, Ser. Mat. Fiz.*, *197*, 1312–1314, doi:1971DoSSR.197.1312T.

Urbar, J., Z. Nemecek, L. Prech, J. Safrankova, and K. Jelinek (2013), Solar wind modification upstream of the bow shock, *AIP Conf. Proc.*, *1539*, 438–441, doi:10.1063/1.4811079.